analytical chemistry

pubs.acs.org/ac Article

# Signal-Amplified Detection of the Tumor Biomarker FEN1 Based on Cleavage-Induced Ligation of a Dumbbell DNA Probe and Rolling Circle Amplification

Bingzhi Li,* Anqi Xia, Siying Xie, Lei Lin, Zhirun Ji, Tiying Suo, Xing Zhang,* and He Huang*

Cite This: *Anal. Chem.* 2021, 93, 3287−3294 Read Online

ACCESS | Metrics & More | Article Recommendations | Supporting Information

**ABSTRACT:** Flap endonuclease 1 (FEN1), an endogenous nuclease with the ability to cleave the 5′ overhang of branched dsDNA, is of significance in DNA replication and repair. The overexpression of FEN1 is common in cancer because of the ubiquitous upregulation of DNA replication; thus, FEN1 has been recognized as a potential biomarker in oncological investigations. However, few analytical methods targeting FEN1 with high sensitivity and simplicity have been developed. This work developed a signal-amplified detection of FEN1 based on the cleavage-induced ligation of a dumbbell DNA probe and rolling circle amplification (RCA). A flapped dumbbell DNA probe (FDP) was rationally designed with a FEN1 cleavable flap at the 5′ end. The cleavage generated a nick site with juxtaposed 5′ phosphate and 3′ hydroxyl ends, which were linkable by T4 DNA ligase to form a closed dumbbell DNA probe (CDP) with a circular conformation. The CDP functioned as a template for RCA, which produced abundant DNA that could be probed using SYBR Green I. The highly sensitive detection of FEN1 with a limit of detection of 15 fM was achieved, and this method showed high specificity, which enabled the quantification of FEN1 in real samples. The inhibitory effects of chemicals on FEN1 were also evaluated. This study represents the first attempt to develop an FEN1 assay that involves signal amplification, and the novel biosensor method enriches the tools for FEN1-based diagnostics.

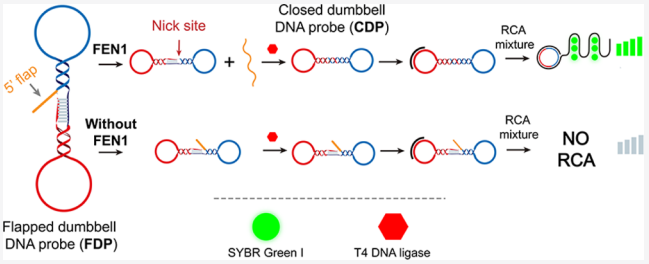




## 1. INTRODUCTION

The critical role of biomarkers in disease diagnosis and prognosis has been universally recognized, and the advantage of accurate biomarker detection is relevant for the development of precision medicine.[1−3] Flap endonuclease 1 (FEN1) is generated by DNA polymerase and primase during Okazaki fragment maturation.[4−6] FEN1 is crucial for RNA and DNA primer removal during lagging-strand DNA synthesis, and it plays key roles in DNA replication and repair.[7,8] As cancer cells exhibit uncontrolled growth, they tend to replicate rapidly in the human body, resulting in the overexpression of DNA polymerase, which in turn leads to FEN1 overexpression.[9−11] Minimal differentiation can lead to diverse FEN1 protein levels in non-small-cell lung-cancer tissues.[12] It has also been reported that high FEN1 levels correlated with aggressive breast cancer, poor survival, and epithelial ovarian cancer.[9] Therefore, FEN1 has the potential for use as a cancer marker for determining the location, diagnosis, and prognosis of cancers.[5,13,14]

Currently, there has been limited progress toward the development of analytical techniques to detect FEN1. Although FEN1 can be detected using diverse conventional assays, including Western blotting and ELISA,[15,16] the assay performance cannot fulfill the demand for precise detection in clinical applications. Recently, a few emerging biosensors have been proposed, for example, Lu et al. investigated a system composed of graphene oxide (GO) and flapped DNA probes for the detection of FEN1 in live cells.[17] Wei et al. utilized a combination of gold nanoparticles, functional DNA, and organic dyes to quantify FEN1 levels.[18] The two assays have significantly simplified the analytical procedures for FEN1 detection; however, both attempts require the consumption of fluorescent labels or lab-made nanomaterials, which may lead to increased cost and detection instability. Additionally, all the current FEN1 assays were developed by directly reading the enzymatic activity of FEN1, resulting in limited sensitivity because of the lack of signal transduction and amplification. Therefore, analytical methods with increased performance and decreased cost are highly desirable.

The application of functional nucleic acids and DNA nanotechnology is currently an attractive topic in chemistry and life sciences.[19−22] Based on the sequence programmability of DNA, its conformation and function can be rationally

Received: December 16, 2020
Accepted: January 22, 2021
Published: February 2, 2021

**Scheme 1. Schematic Illustration of FEN1 Activity and the Mechanism of Biosensor**[a]

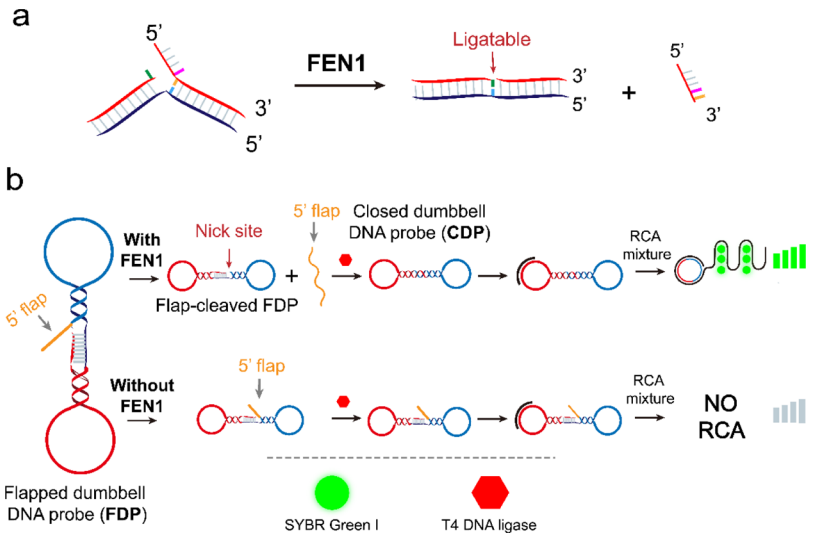


[a](a) Enzymatic activity of FEN1. (b) Sensing mechanism of this method. FEN1 cleaves the 5′ flap of the FDP, exposing a ligatable domain similar to a nick site. A CDP is generated by T4 DNA ligase, RCA is initiated, and the products are probed with SYBR green I (SGI).

designed for recognition,[23,24] catalysis,[25] and computing.[26−28] Rationally designed DNA probes can be used as recognition elements to recognize analytes ranging from metal ions to microorganisms.[29−33] In particular, through their capacity to produce large quantities of nucleic acid fragments under facile conditions,[34] isothermal amplifications such as rolling circle amplification (RCA),[35,36] exponential isothermal amplification (EXPAR),[37] and recombinase polymerase amplification (RPA)[38] have significantly improved the performance of nucleic acid-involved biosensors. To the best of our knowledge, biosensors targeting FEN1 that integrate rationally designed DNA probes and signal amplification have not been reported. Therefore, it is worth attempting to improve the performance of FEN1 biosensors by applying functional nucleic acids.

In this work, we developed a sensing system for the detection of FEN1 that involves RCA. A flapped dumbbell DNA probe (FDP) was rationally designed for the recognition of FEN1 and the transduction of FEN1-induced cleavage signals. The flap hanging over the 5′ terminus of the FDP is cleaved by FEN1, leaving a nick site that can be ligated by T4 DNA ligase. Ligation closes the dumbbell DNA probes, allowing them to be used as a template to initiate RCA. This method is the first attempt to apply signal amplification in the detection of FEN1, which is the result of the rational design of DNA probes and reaction circuits based on the activity of the target. This investigation successfully increased the sensitivity of FEN1 detection to the femtomolar level, thereby enriching the analytical tools for FEN1-based clinical and basic science applications.

## 2. METHODS

**2.1. Materials.** Oligonucleotides were synthesized and purified by Sangon Biotech (Shanghai, China), and their sequences are listed in Table S1. T4 DNA ligase, phi29 DNA polymerase, dNTPs, SYBR Green I (SGI), and chemical reagents for the preparation of buffers were obtained from Sangon Biotech (Shanghai, China). FEN1 was supplied by BBI (Shanghai, China). Aurintricarboxylic acid was purchased from Sigma-Aldrich (MO, USA), and FEN1-IN-1 was obtained from MedChemExpress (Monmouth Junction, NJ, USA). Human brain tissue lysates (normal and tumor) were purchased from Novus Biologicals (CO, U.S.A.). Ultrapure water was prepared using a Millipore Milli-Q system (MA, U.S.A.), and the water was pretreated with diethyl pyrocarbonate (DEPC, BBI, Shanghai, China) to deactivate the DNases and RNases before use in DNA-related experiments.

**2.2. FEN1 Detection.** For the detection of FEN1, FDP (10 $\mu$L, 10 nM), 10 $\mu$L of the test sample, and 30 $\mu$L of reaction buffer (15 mM KCl, 30 mM Tris−HCl, 15 mM $(NH_4)_2SO_4$, and 3 mM $MgSO_4$, pH 8.8) were mixed and incubated at 37 °C for 30 min. Afterward, T4 DNA ligase (1 $\mu$L, 5 U/$\mu$L) in the corresponding 1× reaction buffer was added to the solution, followed by incubation at 22 °C for 40 min. Then, primers and 5 $\mu$L of RCA mixture (2 U of phi29 DNA polymerase, 1 mM dNTPs, 1 × phi29 reaction buffer, and 1 × SGI) were added to the reaction to initiate the RCA reaction. After reaction at 30 °C for RCA, fluorescence was measured using an F-7100 fluorescence spectrometer (Hitachi, Japan) with excitation at $\lambda$ = 497 nm. Rapid, high-throughput detection was conducted using a Synergy H-1 plate reader (Biotek, U.S.A.) with excitation and emission at 497 and 530 nm, respectively.

## 3. RESULTS AND DISCUSSION

**3.1. Principle of the Developed Biosensor in the Sensing of FEN1.** FEN1 is an endonuclease that specifically cleaves the 5′ overhang of branched DNA, thus the sensing system was designed based on its enzymatic activity.[39] As shown in Scheme 1a, when a 3′ flap with a single nucleotide exists (the green nucleotide), the 3′ flap can fill the gap generated after the FEN1-induced cleavage (hybridize with the blue nucleotide), forming a ligatable structure. Rationally designed FDPs with a 5′ flap and a 3′ flap with a single nucleotide were used for the recognition of FEN1. In the presence of FEN1, the 5′ flap is excised, exposing a 5′ phosphate group. Because of the stabilization of the DNA scaffold, the 5′ phosphate and the 3′ flap with the hydroxyl terminus are approached in the juxtaposition, forming a nick site that is ligatable by T4 DNA ligase.[40,41] After ligation, a


https://dx.doi.org/10.1021/acs.analchem.0c05275
Anal. Chem. 2021, 93, 3287−3294

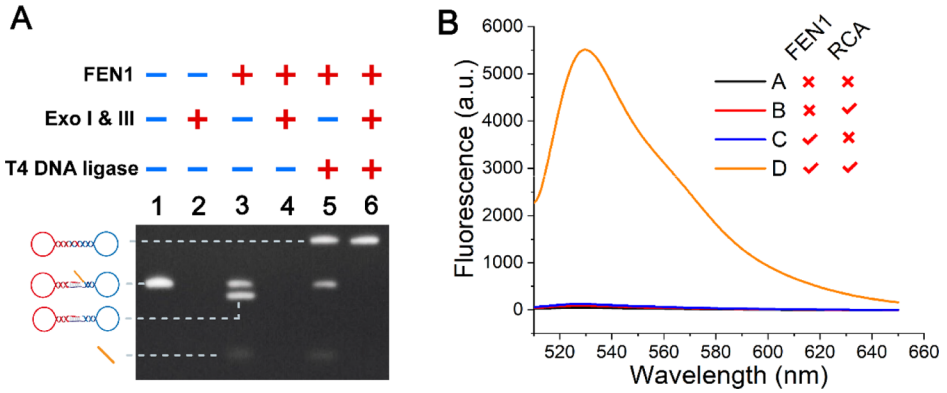


**Figure 1.** Proof-of-concept test of the biosensor. (A) Native-PAGE verification. The concentrations of FDP, FEN1, Exo I, Exo III, and T4 DNA ligase were 10 $\mu$M, 10 nM, 2 U/$\mu$L, 2 U/$\mu$L, and 5 U/$\mu$L, respectively. The times for cleavage, ligation, and Exo digestion were 20 min, 20 min, and 1 h, respectively. (B) Fluorescence response of this method under various conditions. The final concentrations of FDP and FEN1 were 2 nM and 1 pM, and the RCA was conducted by adding the RCA mixture, as described in the Methods section, and incubating for 30 min.

closed dumbbell DNA probe (CDP) is formed, which yields a circular conformation without a free terminus. Afterward, an RCA mixture composed of primers, phi29 DNA polymerase, dNTPs, and SGI, was added to the system. By initiating the RCA reaction, long-chain DNA with repetitive domains complementary to the template is generated and the SGI can be inserted into the self-hybridized domains of the DNA and generate intense green fluorescence for quantification. In contrast, when no FEN1 is in the system, the flap is cleaved and ligation occurs. As a result, no long-chain DNA is generated because of the lack of a template for DNA extension. Following this diagram, more FEN1 leads to higher fluorescence, yielding an activatable biosensor for FEN1 detection.

**3.2. Proof-Of-Concept Test.** We used the gel electrophoresis and fluorescence spectra to verify the design of the sensing scheme. In Figure 1a, six lanes can be seen in the gel image from native polyacrylamide gel electrophoresis (native-PAGE), which is the gold standard for analyzing the length, bending, and flexibility of nucleic acids.[34,42,43] Lane 1 contains a single bright band, which represents the FDP band that serves as a marker. The band uniformity observed in Lane 1 indicates that annealing of the ssDNA generated a uniform FDP. Lane 2 shows that the addition of exonuclease (Exo) I and III to the sample resulted in lack of a visible band. Exo I and III can shred the DNA with exposed 3′ or 5′ termini,[44−46] and the results in Lane 2 can be ascribed to the FDP degradation catalyzed by Exo I and III. After mixing the FDP and a small amount of FEN1 (Lane 3), three bands were recorded. The upper band had a migration speed similar to that of the marker FDP, the middle one is assumed to be the flap-cleaved dumbbell DNA, and the lowest band with the weakest fluorescence is assumed to be the dissociative flap. When Exo I and III were used to treat the sample of Lane 3 and separate it from Lane 4, no apparent bands appeared, indicating that both the cutoff flap and the dumbbell DNA are cleaved thoroughly, similar to the results in Lane 2, confirming that FEN1 is capable of cleaving the FDP with a flapped 5′ end. Then, in Lane 5, the combination of FDP, FEN1, and T4 DNA ligase resulted in three bands in the gel. The upper band is believed to represent CDP produced by the ligation. Similar to the band in Lane 3, the middle band had a migration speed similar to that of the marker and was speculated to be the FDP, and the lowest band was assumed to be the dissociative flap, as was the lowest band in Lane 3. Finally, the addition of Exo I and III to the Lane 5 sample led to the disappearance of the two lower bands; in contrast, the upper band was not influenced by Exo I and III, implying that CDP was generated, given that it is resistant to Exo I and III. In general, this experiment demonstrates that FEN1 can cleave the 5′ flap of FDPs, and the CDP is generated with the aid of T4 DNA ligase.

To verify the RCA procedure, we used agarose gel electrophoresis, which is an effective assay for the separation and imaging of DNA fragments of size 100 to 25k bp.[47,48] Higher concentrations of FEN1 were mixed with FDP, followed by the addition of T4 DNA ligase and RCA mixture. After incubation, the samples were analyzed by agarose gel electrophoresis. As shown in Figure S1, the results visually revealed DNA with a large size, which was recognized as a product of RCA reaction. In addition, the quantity of RCA products positively correlated with the FEN1 concentration, further supporting FEN1-induced cleavage and T4 DNA ligase-mediated formation of looped dumbbell DNA. Moreover, the image of agarose gel electrophoresis and images of native-PAGE reinforced with each other demonstrate that after FEN1 cleavage and T4 DNA ligase connection, the DNA with the lowest migration speed in native-PAGE was a circular DNA that could act as a template for the RCA reaction.

Furthermore, we utilized fluorescence spectra to verify the sensing scheme (Figure 1b). When neither FEN1 nor the RCA mixture was added to the reaction, low fluorescence was recorded (black curve), indicating that the template, primer, and T4 DNA ligase were not able to induce significant fluorescence. Adding the RCA mixture without FEN1 (red curve) has also led to weak fluorescence recording, as without cleavage, the FDP was not capable of functioning as a template for RCA. After introducing only FEN1 (blue curve), no significant fluorescence was recorded, demonstrating that without the RCA mixture, CDP did not cause intense fluorescence enhancement. When both FEN1 and RCA mixture were added, significant emission centered at 530 nm was recorded (orange curve). This demonstrated that only when both FEN1 and RCA mixture were input into the system would a complete chain reaction take place to generate a sensing signal. With the assistance of gel electrophoresis and fluorescence spectroscopy, we can conclude that after the chain reaction was caused by FEN1, T4 DNA ligase, and the RCA


https://dx.doi.org/10.1021/acs.analchem.0c05275
Anal. Chem. 2021, 93, 3287−3294

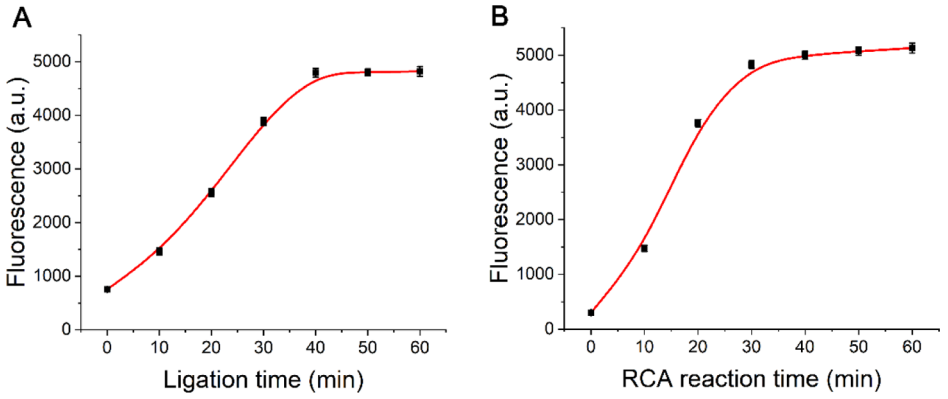


**Figure 2.** Optimization of sensing conditions. (a) Relationship between the ligation time and fluorescence of the total reaction. Experimental details: 5 pM of FEN1 was incubated with FDP for 30 min and then 5 U of T4 DNA ligase was added and incubated at 22 °C for different time intervals. Afterward, the RCA reaction was conducted by adding the RCA master mix and incubating at 37 °C for 30 min. (b) Relationship between the RCA reaction time and the fluorescence of the total reaction. Experimental details: 5 pM of FEN1 was incubated with FDP for 30 min and then 5 U of T4 DNA ligase was added and incubated at 22 °C for 40 min. Afterward, the RCA reaction was conducted by adding the RCA master mix and incubating at 37 °C for different time intervals.

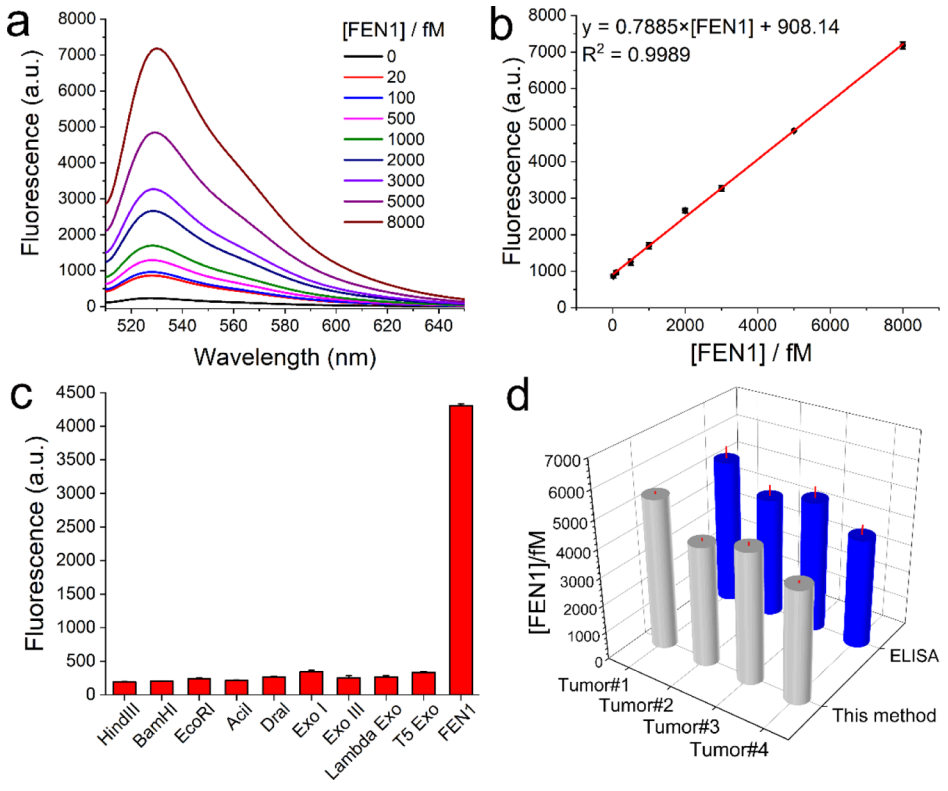


**Figure 3.** Performance of this method in the detection of FEN1. (A) Fluorescence spectra detected by the sensing system upon addition of different concentrations of FEN1. (B) Linear relationship between the FEN1 concentrations and the fluorescent signal. (C) Selectivity of this method toward FEN1. The concentrations of all the interferents were all 20 U/$\mu$L, while that of FEN1 was 5 pM. (D) FEN1 quantification in tumor samples was determined using this method and commercial ELISA kits. All the analyses were conducted following the protocols described in the Methods section. The error bars indicate the standard deviation of three replicate determinations.

mixture, fluorescence is visible, verifying the feasibility of this method in the detection of FEN1.

**3.3. Optimization of Sensing Conditions.** Under the proposed sensing scheme, the ligation process and RCA reaction are key processes influencing the biosensor performance. According to the conditions in previous reports, we arbitrarily mixed 10 nM of FDP with 5 pM of FEN1 for 30 min, and then subsequently investigated the influence of ligation and RCA reaction on the final readout. A constant concentration of FDP was treated with different amounts of T4 DNA ligase for 1 h, followed by the same RCA procedure. As shown in Figure S2, when the amount of T4 DNA ligase was more than 5 U (inclusive), the system fluorescence stopped increasing, indicating that 5 U of T4 DNA ligase was the minimum amount to fully ligate the FDPs in this experimental setting. Different ligation time intervals were then evaluated, followed by a constant RCA reaction. As presented in Figure 2a, fluorescence climbed synchronously until reaching a


https://dx.doi.org/10.1021/acs.analchem.0c05275
Anal. Chem. 2021, 93, 3287−3294

Table 1. Comparison between This Work and Recent Reports on the Analytical Methods Targeting FEN1

| detection signal | comment | LOD | linear range | refs |
|---|---|---|---|---|
| fluorescent | graphene oxide and dye-labeled DNA-formed nanocomposite. | 0.38 pM | 0.2−100 pM | 17 |
| fluorescent | DNA and gold nanoparticle-assembled nanoparticle. | 0.007 U | 0.05−2 U | 18 |
| **fluorescent** | **detection based on cleavage-induced ligation of dumbbell DNA probe and RCA.** | 15 fM | 20−**8000 fM** | **this work** |

plateau after 40 min, demonstrating that 40 min of ligation is sufficient to completely link the flap-cleaved FDPs. As is shown in Figure 2b, before reaching a peak at 30 min, fluorescence was nearly proportional to the duration of the RCA reaction. Only a slight fluorescence increase occurred when the RCA reaction was extended after 30 min, which indicated that 30 min was sufficient to complete the rapid amplification. These experiments demonstrated that the optimal ligation duration was 40 min and the optimal RCA reaction duration was 30 min; therefore, these conditions were adopted in further analysis.

**3.4. Detection of FEN1.** Various concentrations of FEN1 were added to the reaction system, and the final fluorescence intensity of the detection channel was recorded. As shown in Figure 3a, the more the FEN1 was added, the higher the fluorescence was recorded. With increasing FEN1 in the system, more cleavage-induced ligation took place, resulting in greater amounts of CDP functioning as templates for amplification. In Figure 3b, the fluorescence change was proportional to the concentrations of FEN1, and a linear relationship ($y = 0.7885 \times [\mathrm{FEN1}] + 908.14$, $R^2 = 0.9989$) from 20 to 8000 fM was observed. According to the rule of $3\sigma$/slope, the limit of detection (LOD) was calculated as 15 fM. It should be noted that the cleavage of the 5′ overhang depends on the activity of FEN1; thus, the amount of FEN1 can also be expressed in active units.[18] However, the FEN1 used in our research was supplied in mass units, so we used the concentration unit in this report. Compared with the FEN1-responsive nanobiosensor composed of graphene oxide,[17] ∼20-fold improvement in sensitivity was achieved. Comparisons between this method and the existing FEN1 biosensors are listed in Table 1, and it can be seen that this method first achieved sensitivity at the femtomolar level without the use of organic fluorescent labels. In particular, the procedures mainly involve sample addition and isothermal incubation, which possess the advantages of simplicity and convenience. Moreover, all the enzymes, reagents, and oligonucleotides can be commercially supplied, which avoid the instability derived from the synthesis of home-made nanomaterials.

The selectivity of this method toward FEN1 was evaluated using a wide range of interferents. Since FEN1 is an endonuclease, selected endonucleases (HindIII, BamHI, EcoRI, AciI, and DraI) and exonucleases (Exo I, Exo III, Lambda Exo, and T5 Exo) were added to the reaction system to verify the selectivity of this method. These nucleases or enzymes with similar functions commonly exist in testing samples, and they are also widely used in the pretreatment of certain cellular extracts. As shown in Figure 3c, only FEN1 induced a high fluorescence response, which is consistent with the design of the biosensor. The interferents were not able to mediate the removal of the 5′ flap of FDP, thus, no downstream reactions could take place. These results indicated the high selectivity of the method toward FEN1, which is rooted in the rational design of FDPs based on the enzymatic activity of FEN1.

To test the specificity of FEN1 in real samples, we conducted recovery tests by spiking known quantities of FEN1 into the nucleoproteins extracted from cultured HeLa cells and glioma samples donated by volunteers from Nanjing Hospital of Chinese Medicine. The linear relationship described in Figure 3B was used to measure FEN1 concentrations. Table 2 shows the results of this experiment,

Table 2. Results of the Recovery Test Involving Spiking FEN1 into Real Samples Extracted from Cultured Cells and Clinical Samples

| sample | content (fM) | spiked (fM) | detected (fM) | recovery (%) | RSD ($n$ = 6, %) |
|---|---|---|---|---|---|
| HeLa cells | 3342.1 | 1000 | 4398.7 | 105.7 | 1.9 |
| | | 2000 | 5363.9 | 101.1 | 2.2 |
| | | 3000 | 6272.3 | 97.7 | 1.7 |
| glioma | 4271.4 | 1000 | 5325.1 | 105.3 | 2.0 |
| | | 2000 | 6317.3 | 102.3 | 1.6 |
| | | 3000 | 7476.5 | 106.84 | 1.9 |

including both the non-spiked and spiked samples. The recovery ranges from 97.7 to 106.84%, meeting the requirement for chemical analysis. These results indicated that the calibration curve obtained under buffer conditions can be used in the real sample analysis with permutable errors, and further imply that this method possesses high specificity under the challenge of complicated biometrics in the cell extracts. Moreover, 1.6−2.2% of RSD revealed the precision of this method, which has a high potential to be robustly applied in clinical analysis.

To test the accuracy of this biosensor in the detection of FEN1, we analyzed FEN1 in gliomas from four patients using our method and ELISA, respectively. As shown in Figure 3d, the results obtained by the two assays were almost identical. The correlations between the quantification results were analyzed further, and it was found that the concentrations of FEN1 determined by our method and ELISA were directly proportional (Figure S3). ELISA is a general method for the detection of antigens based on immunity, while our method was developed based on the enzymatic activity of FEN1. In general, the consistency between the two assays indicates that our method can facilitate the accurate and specific detection of FEN1 in real clinical samples. Furthermore, FEN1 levels in tissue lysates of both normal human brains and brains with tumors were analyzed using this method. It was found that the tumor tissue expressed more FEN1 than the normal tissue (Figure S4), which is in line with the previous reports.[49,50] Notably, due to the low abundance of FEN1 in whole brain tissue lysate samples, ELISA was not sensitive enough to conduct the analysis. Therefore, our method has a high potential for detecting low concentrations of FEN1 in real samples, which is critical for clinical diagnosis.

**3.5. Inhibition Assay.** Because of the role of FEN1 in cell proliferation and oncogenesis, it has been recognized as a potential drug target.[4,51] The inhibitory effect of chemicals on


https://dx.doi.org/10.1021/acs.analchem.0c05275
Anal. Chem. 2021, 93, 3287−3294

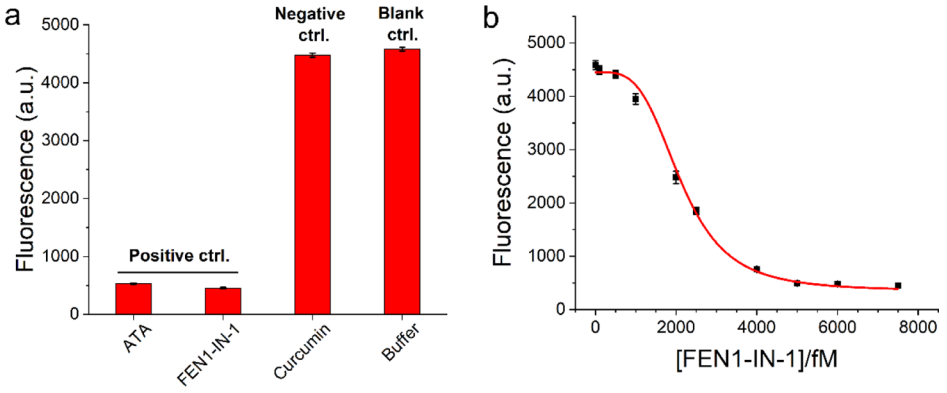


**Figure 4.** FEN1 inhibition assays. (a) Evaluation of the inhibitory effect of different chemicals on FEN1. FEN1 (5 pM) and the indicated chemicals (5 pM) were mixed for 20 min before the addition of FDP. (b) Relationship between the concentration of FEN-IN-1 and the fluorescent readout. FEN1 (5 pM) and different concentrations of FEN-IN-1 were mixed for 20 min prior to downstream reactions. Analyses were conducted according to the standard protocol described in the Methods section, and error bars represent the standard deviation of three replicate experiments.

FEN1 can be determined by *in vivo* and *in vitro* assays. Although *in vivo* assays are the best choice to reflect the activity of candidate chemicals in living cells or animals, the diversity of biological systems, high cost, and specialized experimental skills may pose technical barriers to drug screening.[52,53] The development of facile *in vitro* assays could significantly increase the efficiency of drug discovery, enabling rapid preliminary screening to narrow down candidates.[54,55] We explored the possibility of applying it in the evaluation of FEN1 inhibitors. Using ATA and FEN1-IN-1 as positive controls,[17,18] curcumin as a negative control, and buffer as a blank control, inhibition assays were conducted. As shown in Figure 4a, the fluorescence was weak in the presence of inhibitors, which indicated that ATA and FEN1-IN-1 have strongly inhibited the activity of FEN1, thus blocking the whole reaction chain by intercepting the cleavage-induced ligation. In contrast, without an inhibitor, strong fluorescence was observed in the blank and negative control conditions. Besides, different concentrations of FEN1-IN-1 were incubated with the same quantity of FEN1, followed by the same analyses. As shown in Figure 4b, the fluorescence decreased with increasing FEN1-IN-1 concentration, and the half-maximal inhibitory concentration (IC50) was calculated as 2.12 pM by fitting the curve. These tests show that the application of this biosensor can be extended to the *in vitro* screening and evaluation of FEN1 inhibitors.

## 4. CONCLUSIONS

In this study, cleavage-induced ligation of a dumbbell DNA probe and RCA were integrated for the signal-amplified detection of the tumor biomarker FEN1. FEN1 cleavage leaves 5′ phosphate at the cleaving site, which forms a ligatable nick site. T4 DNA ligase was used for the formation of CDP, which can function as a template to trigger the RCA reaction. The RCA reaction was subsequently used to achieve signal amplification, improving the sensitivity for FEN1 sensing to the femtomolar level. The specificity of this biosensor has been evaluated using real samples, and similar results were observed in clinical samples as compared with a commercial assay. Our work proposed a new method for FEN1 sensing by rationally designing a DNA reaction network rooted in the activity of FEN1. Notably, a brunched DNA conformation similar to the FEN1-recognizable structure could be generated during the strand displacement of the RCA reaction; however, our tests indicated that the long-chain DNA can still be produced without significant influence. Our assumption of this interesting phenomenon is that the phi29 DNA polymerase could inhibit the approach between the DNA and FEN1, and FEN1 may not stably bind to its substrate during the rapid RCA process. Further investigation will be conducted to reveal the underlying mechanism of this new finding in our future work. In summary, it not only provides an improved method to achieve FEN1 recognition and signal amplification of FEN1 but also offers an improved approach for use in FEN1-related oncological investigations.

## ■ ASSOCIATED CONTENT

### Supporting Information

The Supporting Information is available free of charge at https://pubs.acs.org/doi/10.1021/acs.analchem.0c05275.

Experimental details of gel electrophoresis, extraction of nucleoproteins, and ELISA; DNA sequences; image of agarose gel electrophoresis; optimization of the T4 DNA ligase dose; analysis of FEN1 by ELISA and this method; and FEN1 level in human brain whole tissues (PDF)

## ■ AUTHOR INFORMATION


### Corresponding Authors

**Bingzhi Li** − *School of Food Science and Pharmaceutical Engineering, Nanjing Normal University, Nanjing 210023, China*; orcid.org/0000-0002-5533-2147; Email: bingzhili@njnu.edu.cn

**Xing Zhang** − *School of Food Science and Pharmaceutical Engineering, Nanjing Normal University, Nanjing 210023, China*; Email: zhangxing@njnu.edu.cn

**He Huang** − *School of Food Science and Pharmaceutical Engineering, Nanjing Normal University, Nanjing 210023, China*; Email: huangh@njnu.edu.cn

### Authors

**Anqi Xia** − *School of Food Science and Pharmaceutical Engineering, Nanjing Normal University, Nanjing 210023, China*

**Siying Xie** − *School of Food Science and Pharmaceutical Engineering, Nanjing Normal University, Nanjing 210023, China*

**Lei Lin** − *School of Environment, Nanjing Normal University, Nanjing 210023, China*




https://dx.doi.org/10.1021/acs.analchem.0c05275
*Anal. Chem.* 2021, 93, 3287−3294

**Zhirun Ji** − *School of Food Science and Pharmaceutical Engineering, Nanjing Normal University, Nanjing 210023, China*

**Tiying Suo** − *School of Food Science and Pharmaceutical Engineering, Nanjing Normal University, Nanjing 210023, China*

Complete contact information is available at: https://pubs.acs.org/10.1021/acs.analchem.0c05275

### Notes

The authors declare no competing financial interest.

## ■ ACKNOWLEDGMENTS

This work was supported by grants from the Natural Science Foundation of Jiangsu Province (no. BK20200718 to B.L. and BK20200728 to X.Z.), the National Natural Science Foundation of China (no. 22007049), the Natural Science Foundation of Jiangsu Higher Education Institutions of China (20KJB350010 to B.L.), and the Scientific Research Start-Up Funding for Nanjing Normal University Introduced Talents (184080H202B246). T.Y.S. acknowledges funding from the Postgraduate Research & Practice Innovation Program of Jiangsu Province (KYCX20_1261).

## ■ REFERENCES

(1) Sveen, A.; Kopetz, S.; Lothe, R. A. *Nat. Rev. Clin. Oncol.* **2020**, *17*, 11−32.
(2) Morel, D.; Jeffery, D.; Aspeslagh, S.; Almouzni, G.; Postel-Vinay, S. *Nat. Rev. Clin. Oncol.* **2020**, *17*, 91−107.
(3) Fan, C. M.; Wang, J. P.; Tang, Y. Y.; Zhao, J.; He, S. Y.; Xiong, F.; Guo, C.; Xiang, B.; Zhou, M.; Li, X. L.; Li, Y.; Li, G. Y.; Xiong, W.; Zeng, Z. Y. *Canc. Sci.* **2019**, *110*, 2180−2188.
(4) Ba, S.; Zhang, H.; Lee, J. Y.; Wu, H.; Ye, R.; Huang, D.; Li, T. *Bioorg. Med. Chem.* **2016**, *24*, 1988−1992.
(5) Tsutakawa, S. E.; Classen, S.; Chapados, B. R.; Arvai, A. S.; Finger, L. D.; Guenther, G.; Tomlinson, C. G.; Thompson, P.; Sarker, A. H.; Shen, B.; Cooper, P. K.; Grasby, J. A.; Tainer, J. A. *Cell* **2011**, *145*, 198−211.
(6) Xin, X.; Wen, T.; Gong, L.-B.; Deng, M.-M.; Hou, K.-Z.; Xu, L.; Shi, S.; Qu, X.-J.; Liu, Y.-P.; Che, X.-F.; Teng, Y.-E. *Front. Oncol.* **2020**, *10*, 425.
(7) Flach, K. D.; Periyasamy, M.; Jadhav, A.; Dorjsuren, D.; Siefert, J. C.; Hickey, T. E.; Opdam, M.; Patel, H.; Canisius, S.; Wilson, D. M.; Donaldson Collier, M.; Prekovic, S.; Nieuwland, M.; Kluin, R. J. C.; Zakharov, A. V.; Wesseling, J.; Wessels, L. F. A.; Linn, S. C.; Tilley, W. D.; Simeonov, A.; Ali, S.; Zwart, W. *Cancer Res.* **2020**, *80*, 1914−1926.
(8) He, L.; Yang, H.; Zhou, S.; Zhu, H.; Mao, H.; Ma, Z.; Wu, T.; Kumar, A. K.; Kathera, C.; Janardhan, A.; Pan, F.; Hu, Z.; Yang, Y.; Luo, L.; Guo, Z. *DNA Repair* **2018**, *63*, 1−9.
(9) Abdel-Fatah, T. M. A.; Russell, R.; Albarakati, N.; Maloney, D. J.; Dorjsuren, D.; Rueda, O. M.; Moseley, P.; Mohan, V.; Sun, H.; Abbotts, R.; Mukherjee, A.; Agarwal, D.; Illuzzi, J. L.; Jadhav, A.; Simeonov, A.; Ball, G.; Chan, S.; Caldas, C.; Ellis, I. O.; Wilson, D. M.; Madhusudan, S. *Mol. Oncol.* **2014**, *8*, 1326−1338.
(10) Li, J. L.; Wang, J. P.; Chang, H.; Deng, S. M.; Du, J. H.; Wang, X. X.; Hu, H. J.; Li, D. Y.; Xu, X. B.; Guo, W. Q.; Song, Y. H.; Guo, Z.; Sun, M. X.; Wu, Y. W.; Liu, S. B. *Cancer Med.* **2019**, *8*, 7774−7780.
(11) Williams, R. S.; Kunkel, T. A. *Cell* **2011**, *145*, 171−172.
(12) Zhang, K.; Keymeulen, S.; Nelson, R.; Tong, T. R.; Yuan, Y.-C.; Yun, X.; Liu, Z.; Lopez, J.; Raz, D. J.; Kim, J. Y. *Am. J. Surg. Pathol.* **2018**, *188*, 242−251.
(13) Zhang, Y.; Liu, X.; Liu, L.; Chen, J.; Hu, Q.; Shen, S.; Zhou, Y.; Chen, S.; Xue, C.; Cui, G.; Yu, Z. *Dis. Markers* **2020**, *2020*, 1−17.
(14) Lam, J. S.; Seligson, D. B.; Yu, H.; Li, A.; Eeva, M.; Pantuck, A. J.; Zeng, G.; Horvath, S.; Belldegrun, A. S. *BJU Int.* **2006**, *98*, 445−451.
(15) He, L.; Zhang, Y.; Sun, H.; Jiang, F.; Yang, H.; Wu, H.; Zhou, T.; Hu, S.; Kathera, C. S.; Wang, X.; Chen, H.; Li, H.; Shen, B.; Zhu, Y.; Guo, Z. *EBioMedicine* **2016**, *14*, 32−43.
(16) Ma, L.; Cao, X.; Wang, H.; Lu, K.; Wang, Y.; Tu, C.; Dai, Y.; Meng, Y.; Li, Y.; Yu, P.; Man, S.; Diao, A. *J. Agric. Food Chem.* **2019**, *67*, 1656−1665.
(17) Zhang, H.; Ba, S.; Mahajan, D.; Lee, J. Y.; Ye, R.; Shao, F.; Lu, L.; Li, T. *Nano Lett.* **2018**, *18*, 7383−7388.
(18) Wang, C.; Zhang, D.; Tang, Y.; Wei, W.; Liu, Y.; Liu, S. *ACS Appl. Bio Mater.* **2020**, *3*, 4573−4580.
(19) Suo, T.; Sohail, M.; Xie, S.; Li, B.; Chen, Y.; Zhang, L.; Zhang, X. *J. Hazard. Mater.* **2021**, *403*, 123418.
(20) Samanta, D.; Ebrahimi, S. B.; Kusmierz, C. D.; Cheng, H. F.; Mirkin, C. A. *J. Am. Chem. Soc.* **2020**, *142*, 13350−13355.
(21) Liu, J.; Cao, Z.; Lu, Y. *Chem. Rev.* **2009**, *109*, 1948−1998.
(22) Zhao, Z.; Yang, H.; Zhao, W.; Deng, S.; Zhang, K.; Deng, R.; He, Q.; Gao, H.; Li, J. *J. Mater. Chem. B* **2020**, *8*, 3623−3630.
(23) Iliuk, A. B.; Hu, L.; Tao, W. A. *Anal. Chem.* **2011**, *83*, 4440−4452.
(24) Meng, H.-M.; Liu, H.; Kuai, H.; Peng, R.; Mo, L.; Zhang, X.-B. *Chem. Soc. Rev.* **2016**, *45*, 2583−2602.
(25) Willner, I.; Shlyahovsky, B.; Zayats, M.; Willner, B. *Chem. Soc. Rev.* **2008**, *37*, 1153.
(26) Xu, J.; Tan, G. *J. Comput. Theor. Nanosci.* **2007**, *4*, 1219−1230.
(27) Rozen, D. E.; McGrew, S.; Ellington, A. D. *Curr. Biol.* **1996**, *6*, 254−257.
(28) Li, Y.; Teng, X.; Zhang, K.; Deng, R.; Li, J. *Anal. Chem.* **2019**, *91*, 3989−3996.
(29) Li, B.; Chen, Y.; Wang, J.; Lu, Q.; Zhu, W.; Luo, J.; Hong, J.; Zhou, X. *Anal. Chim. Acta* **2019**, *1048*, 168−177.
(30) Li, B.; Xu, L.; Chen, Y.; Zhu, W.; Shen, X.; Zhu, C.; Luo, J.; Li, X.; Hong, J.; Zhou, X. *Anal. Chem.* **2017**, *89*, 7316−7323.
(31) Shen, J.; Zhou, X.; Shan, Y.; Yue, H.; Huang, R.; Hu, J.; Xing, D. *Nat. Commun.* **2020**, *11*, 267.
(32) Liang, M.; Li, Z.; Wang, W.; Liu, J.; Liu, L.; Zhu, G.; Karthik, L.; Wang, M.; Wang, K.-F.; Wang, Z.; Yu, J.; Shuai, Y.; Yu, J.; Zhang, L.; Yang, Z.; Li, C.; Zhang, Q.; Shi, T.; Zhou, L.; Xie, F.; Dai, H.; Liu, X.; Zhang, J.; Liu, G.; Zhuo, Y.; Zhang, B.; Liu, C.; Li, S.; Xia, X.; Tong, Y.; Liu, Y.; Alterovitz, G.; Tan, G.-Y.; Zhang, L.-X. *Nat. Commun.* **2019**, *10*, 3672.
(33) Xiong, Y.; Zhang, J.; Yang, Z.; Mou, Q.; Ma, Y.; Xiong, Y.; Lu, Y. *J. Am. Chem. Soc.* **2019**, *142*, 207−213.
(34) Chen, Y.; Yan, X.; Yang, W.; Wang, J.; Lu, Q.; Li, B.; Zhu, W.; Zhou, X. *J. Chromatogr. A* **2020**, *1624*, 461148.
(35) Bialy, R. M.; Ali, M. M.; Li, Y.; Brennan, J. D. *Chem.—Eur. J.* **2020**, *26*, 5085−5092.
(36) Gao, H.; Zhang, K.; Teng, X.; Li, J. *TrAC, Trends Anal. Chem.* **2019**, *121*, 115700.
(37) Reid, M. S.; Le, X. C.; Zhang, H. *Angew. Chem., Int. Ed.* **2018**, *57*, 11856−11866.
(38) Lobato, I. M.; O'Sullivan, C. K. *TrAC, Trends Anal. Chem.* **2018**, *98*, 19−35.
(39) Lee, C. Y.; Jang, H.; Kim, H.; Jung, Y.; Park, K. S.; Park, H. G. *Microchim. Acta* **2019**, *186*, 330.
(40) Kao, H.-I.; Henricksen, L. A.; Liu, Y.; Bambara, R. A. *J. Biol. Chem.* **2002**, *277*, 14379−14389.
(41) Sharma, S.; Otterlei, M.; Sommers, J. A.; Driscoll, H. C.; Dianov, G. L.; Kao, H.-I.; Bambara, R. A.; Brosh, R. M. *Mol. Biol. Cell* **2004**, *15*, 734−750.
(42) Suo, T.; Sohail, M.; Ma, Y.; Li, B.; Chen, Y.; Zhang, X.; Zhou, X. *Sens. Actuators, B* **2020**, *324*, 128586.
(43) Zhang, K.; Fan, Z.; Li, H.; Zhao, J.; Xie, M. *Anal. Chim. Acta* **2020**, *1104*, 132−139.
(44) Zhang, Y.; Li, Q.-n.; Xiang, D.-x.; Zhou, K.; Xu, Q.; Zhang, C.-y. *Chem. Commun.* **2020**, *56*, 8952−8955.
(45) Lu, L.; Su, H.; Li, F. *Anal. Chem.* **2017**, *89*, 8328−8334.
(46) Zhang, Y.; Xiang, D.; Tang, B.; Zhang, C.-y. *Anal. Chem.* **2017**, *89*, 10439−10445.

(47) Jiang, Y.; Zou, S.; Cao, X. *Sens. Actuators, B* **2017**, *251*, 976−984.
(48) McMaster, G. K.; Carmichael, G. G. *Proc. Natl. Acad. Sci. U.S.A.* **1977**, *74*, 4835−4838.
(49) Chen, Y.-D.; Zhang, X.; Qiu, X.-G.; Li, J.; Yuan, Q.; Jiang, T.; Yang, M. *J. Neuro Oncol.* **2013**, *111*, 145−151.
(50) Nikolova, T.; Christmann, M.; Kaina, B. *Anticancer Res.* **2009**, *29*, 2453−2459.
(51) Guo, E.; Ishii, Y.; Mueller, J.; Srivatsan, A.; Gahman, T.; Putnam, C. D.; Wang, J. Y. J.; Kolodner, R. D. *Proc. Natl. Acad. Sci. U.S.A.* **2020**, *117*, 19415−19424.
(52) Roda, A.; Guardigli, M.; Pasini, P.; Mirasoli, M. *Anal. Bioanal. Chem.* **2003**, *377*, 826−833.
(53) Ramirez, B.; Bickle, Q.; Yousif, F.; Fakorede, F.; Mouries, M.-A.; Nwaka, S. *Expet Opin. Drug Discov.* **2007**, *2*, S53−S61.
(54) Tsai, P.-C.; Lee, S.; Michniak-Kohn, B. *Ther. Deliv.* **2015**, *6*, 1043−1052.
(55) Moffat, J. G.; Rudolph, J.; Bailey, D. *Nat. Rev. Drug Discovery* **2014**, *13*, 588−602.


https://dx.doi.org/10.1021/acs.analchem.0c05275
*Anal. Chem.* 2021, 93, 3287−3294